



Adsorption studies of fluoride on weak base anion exchangers and surface modified strong acid cation exchangers in aqueous medium

Janhavi M. Karekar^a, Ramesh T. Katamble^b, Sanjaykumar V. Divekar^{a,*}

^aDepartment of Chemistry, KLS's Gogte Institute of Technology, Belagavi, 590008 Karnataka, India, Tel. +91 9480398575; Fax: +91 831 2441909; emails: svdivekar@git.edu (S.V. Divekar), vmkarekar@git.edu (J.M. Karekar)

^bDepartment of Chemistry, Govindram Seksaria Science college, Belagavi, 590006 Karnataka, India, email: katamblert111@gmail.com (R.T. Katamble)

Received 17 October 2019; Accepted 13 June 2020

ABSTRACT

The study on removal of fluoride from water is performed by using two anion exchangers and two modified cation exchangers by varying contact time, resin dosage, pH, and initial concentration of fluoride ions. Maximum fluoride removal is possible in the pH range of 4.0–10.0 and removal efficiency reaches maximum, within 60 min for anion exchangers and 120 min for cation exchangers. Among Langmuir and Freundlich isotherms, adsorption data fit well in Freundlich isotherm. The kinetic study suggests adsorption process follows pseudo-second-order reaction kinetics. Among two anion exchangers used for the removal of fluoride Tulsion A-10X (MP) has better fluoride removal efficiency than Amberlyst A-21(MP). However, in the case of modified cation exchangers, Al⁺³ forms of resins have better fluoride removal efficiency than Fe⁺³ forms. It clearly indicates that modified resins can be useful for the removal of fluoride. Desorption study is also carried out on all the resins using 0.1 N NaOH and 0.1 N HCl.

Keywords: Adsorption; Kinetics; Fluoride; Anion exchanger; Cation exchanger

1. Introduction

Fluoride is useful to the human health if its concentration in drinking water is within 1–1.5 mg/L [1] to prevent tooth decay. If the concentration exceeds more than 1.5 mg/L, it may lead to harmful effects like dental fluorosis, skeletal fluorosis, headache, neurological damage, and bone cancer [2]. Fluoride gets added to water naturally through plutonic and volcanic activities and also due to use of fluoride compounds in fertilizer, plastic, glass, and textile dyeing industries [3].

Various techniques have been employed by researchers to reduce fluoride concentration from aqueous medium such as coagulation techniques where in alum sludge [4] and lime [5] are used as coagulants. Fluoride has been

removed by using adsorption processes; by adopting different adsorbents like activated alumina or modified activated alumina [6–8], activated carbon [9,10], bone charcoal [11], chitosan-iron complex [12] and Kanuma mud [13]. Nano adsorbents like nano sized alumina and zirconia modified alumina [14], Fe–Ti oxide [15], γ -Fe₂O₃ nanoparticles [16], polypyrrole/Fe₃O₄ magnetic nanocomposites [17] are also used for the fluoride removal in recent years. In addition to this nanofiltration membranes [18], low pressure reverse osmosis membranes [19], and electro dialysis membrane technologies [20,21] are also employed for fluoride removal.

Ion exchange resins are the most promising materials for removing fluoride from water. Commercially available anion exchange resins, chelating resins and modified chelating resins [22–28], metal ions incorporated cation, and anion

* Corresponding author.

exchange resins [29–34] are effectively used for fluoride removal from the water.

In this study two anion exchangers in Cl^- form and two cation exchangers converted into Al^{+3} and Fe^{+3} forms are used to evaluate their fluoride removal efficiency. The comparison of these resins are made based on their defluoridation efficiency by varying the parameters like contact time, resin dosage, pH, and initial concentration of fluoride ions and the data is studied applying equilibrium isotherms and kinetic models.

2. Experimental

2.1. Materials and methods

The weak base anion exchangers with polyacrylic and polystyrene matrix with polyamine and tertiary amine group are used. Also, strong acid cation exchangers with polystyrene matrix having sulfonic acid group are used. The resins are supplied by Thermax Limited (Pune, India) and Himedia Laboratories Pvt., Ltd., (Mumbai, India). Details of resins used for the study are presented in Table 1.

The analytical grade chemical reagents such as KF, NaOH, HCl, $\text{Al}(\text{NO}_3)_3$, $\text{Fe}(\text{NO}_3)_3$, Tisab III are used. The stock solution of fluoride is prepared by dissolving KF in double-distilled water to get concentration 1,000 mg/L. The stock solution is diluted to get required initial concentration.

Weak base anion exchangers in Cl^- form are used directly for fluoride adsorption studies. The strong acid cation exchangers with Na^+ form are converted into Fe^{+3} and Al^{+3} form by treating with 5% (w/v) $\text{Al}(\text{NO}_3)_3$ or $\text{Fe}(\text{NO}_3)_3$ solutions [30] and are used for the removal of fluoride. The abbreviation of resins is listed in Table 2.

2.3. Methods

2.3.1. Adsorption studies by batch method

The adsorption study of fluoride in aqueous medium using resins is carried out by batch method using Toshiba make thermostatic mechanical shaker. The experiments are performed by varying time, pH, resin dosage, and fluoride concentration to optimize the conditions. The concentrations of fluoride ions in the solution after the adsorption is measured using Thermo Scientific Orion Dual (USA) star

ion selective electrode meter with 9409BN fluoride half-cell electrode in combination with 900100 single junction reference electrode.

For kinetic study, known concentration of fluoride solution of 50 cm^3 is taken in 100 cm^3 volumetric flask with a known quantity of resin and flasks are kept for agitation in the mechanical shaker at 303 K. The concentration of fluoride in the solution is checked after specific time intervals. The amount of fluoride adsorbed on resin is calculated from initial concentration and final concentrations after adsorption in the solution.

Equilibrium study is carried out by taking various known concentrations of fluoride solution (2–14 mg/L) in different flasks with fixed quantity of resin. The flasks are kept for agitation until the equilibrium is attained. The fluoride adsorption capacity (q_e), is found out from Eq. (1):

$$q_e = \frac{V \{C_0 - C_e\}}{m} \quad (1)$$

where C_0 and C_e are the initial and equilibrium concentration of fluoride (mg/L), V is the volume of solution (L), and m is the weight of resin (g).

Distribution coefficient (K_d) at equilibrium is calculated using Eq. (2):

$$K_d = \frac{C_a}{C_e} \quad (2)$$

Table 2
Resin abbreviations

Name of the resin	Abbreviation
Al^{+3} form of Tulsion T-40 (gel)	TT-40-Al
Fe^{+3} form of Tulsion T-40 (gel)	TT-40-Fe
Al^{+3} form of Tulsion T-42 (gel)	TT-42-Al
Fe^{+3} form of Tulsion T-42 (gel)	TT-42-Fe
Tulsion A-10X(MP)	TUL-10
Amberlyst A-21(MP)	AMB-21

Table 1
Characteristics of resins

Resin	Tulsion T-40 (gel)	Tulsion T-42 (gel)	Tulsion A-10X(MP)	Amberlyst A-21(MP)
Matrix structure	Cross linked polystyrene	Cross linked polystyrene	Cross linked polyacrylic	Styrene divinylbenzene
Functional group	Sulfonic acid	Sulfonic acid	Polyamine	Tertiary amine
Ionic form	Sodium	Sodium	Free base	Free base
Particle size (mm)	0.3–1.2	0.3–1.2	0.3–1.2	0.49–0.69
Screen size (US mesh)	16–50	16–50	16–50	22–30
Maximum operating temperature ($^{\circ}\text{C}$)	120–140	120–140	80	100
Total exchange capacity (m eq./mL)	1.8	2.0	2.5	1.3
Moisture content (%)	~50%	42–48	52–55	56–62

where C_a is the concentration of fluoride (mg/L) on the resin after the adsorption.

% Removal efficiency of fluoride ($R\%$) is calculated using the Eq. (3):

$$\%R = \frac{C_a}{C_0} \times 100 \quad (3)$$

2.3.2. Desorption studies

Desorption study is carried by taking 1 g of fluoride adsorbed resins in contact with 50 cm³ of 0.1 N NaOH and 0.1 N HCl solution in flasks. The flasks are agitated in orbital shaker for 2 h and the solution is decanted and analyzed for the residual fluoride content. Desorption of the fluoride is calculated using Eq. (4):

$$\% \text{ Desorption} = \frac{D_F}{A_F} \times 100 \quad (4)$$

where D_F and A_F are the amount of fluoride ion concentration desorbed in the solution and adsorbed on the resin in mg/L, respectively.

3. Result and discussion

3.1. Effect of the various parameters for fluoride removal

3.1.1. Effect of contact time

Fig. 1 shows fluoride removal by using resins with respect to contact time. The study is carried out by using 0.2 g of resin with a 10 mg/L of fluoride ion concentration to understand a minimum time of contact needed to attain maximum removal efficiency. The adsorption increases rapidly in the beginning as the number of sites available for adsorption are more [35]. The maximum removal efficiency is observed within 60 min for both anion exchangers and within 120 min for Fe³⁺ and Al³⁺ form of cation exchangers.

3.1.2. Effect of resin dosage

Effect of resin dosage on the removal efficiency of fluoride is studied by varying the resin quantity ranging between 0.25 and 2.0 g and keeping the fluoride ion concentration constant 10 mg/L. The removal efficiency enhanced with increase in resin dosage as represented in Fig. 2, because the number of available surface sites increased due to which the diffusion of fluoride on the resin for adsorption increased [36]. Beyond 1.5 g of resin quantity, the increase in the removal efficiency remained more or less same.

3.1.3. Influence of pH

pH effect is studied by varying the pH of fluoride solution in the range of 3–12 as pH is an important parameter for adsorption studies. The effect is studied by taking 0.2 g resin with 10 mg/L fluoride solution with different pH values at 303 K. The solution pH is adjusted by using HCl

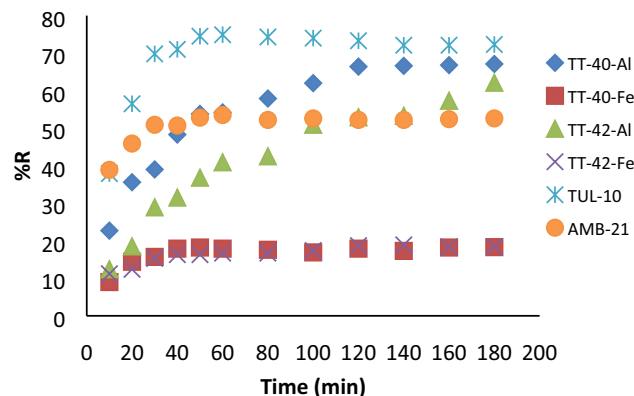


Fig. 1. Effect of contact time on removal of fluoride using resins.

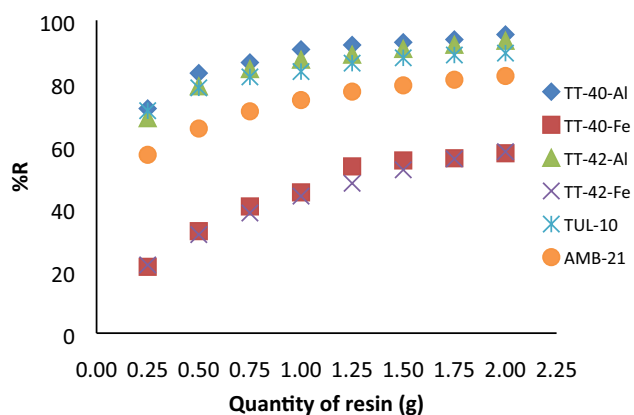


Fig. 2. Effect of resin dosage on the removal of fluoride using resins.

and NaOH solution. Fig. 3 represents the effect of pH on the removal efficiency of fluoride on the resins. The result indicates that the resins can be used to remove fluoride in wide range of pH between 4 and 10. The decrease in removal efficiency below pH 3 on the resins is may be due to formation of HF [37]. The decrease in removal efficiency above pH 10 in case of weak base resin is, as weak base resins get converted to base form which may show less affinity for fluoride ions and in case of strong base resins it may be due to formation of hydroxides of aluminum and iron.

3.1.4. Effect of fluoride ion concentration

The effect of initial concentration of fluoride is studied by varying the concentration of fluoride ions between 2 to 14 mg/L by keeping resin quantity constant. As shown in Fig. 4, the effect of initial concentration of fluoride is negligible on both anion exchangers and cation exchangers in Al³⁺ form. However, in case of cation exchangers in Fe³⁺ form, removal efficiency is less at lower concentrations of fluoride, as the numbers of available sites on resin are more than the ions in the solution. As the concentration increases the number of fluoride ions in the solution increase, however, the number of available sites on resin remain same

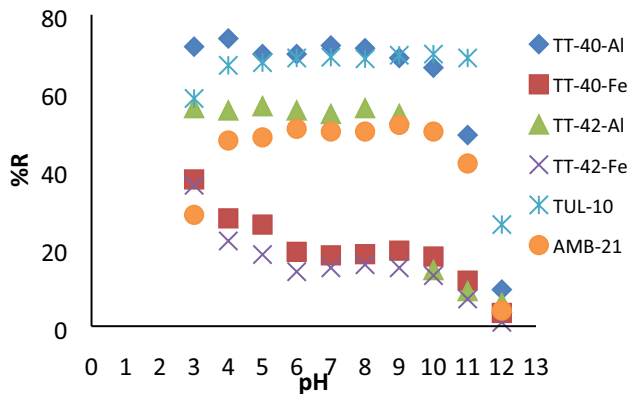


Fig. 3. Effect of pH on removal of fluoride using resins.

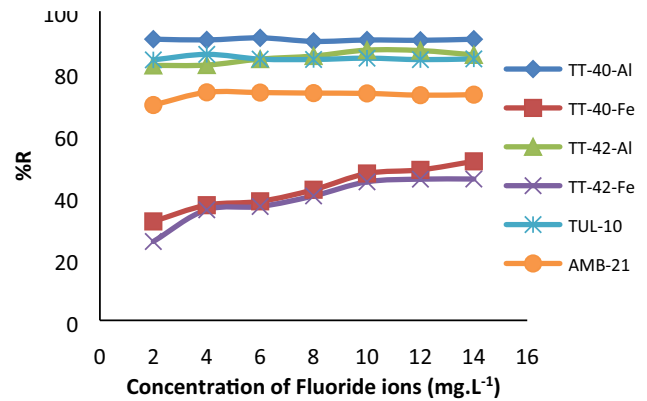


Fig. 4. Effect of concentration of fluoride ions.

so the removal efficiency almost remains constant once the equilibrium concentration is reached [33].

3.2. Adsorption isotherms

Adsorption isotherms relate the interaction of adsorbate with adsorbent. Isotherms help to analyze the relationship between the concentration of adsorbate in the solution and on the adsorbent [38]. Langmuir and Freundlich isotherms are used to analyze the experimental data of fluoride adsorption on the ion exchange resins. The adsorption isotherm parameters are listed in Table 3.

3.2.1. Langmuir adsorption isotherm

The Langmuir equation [39] may be written as:

$$\frac{C_e}{q_e} = \frac{1}{K_L \cdot Q_L} + \frac{C_e}{Q_L} \tag{5}$$

where q_e is the amount of fluoride adsorbed on the resin at equilibrium (mg/g), Q_L is the maximum adsorption capacity (mg/g), K_L is a Langmuir constant which is an affinity term (L/mg), C_e is fluoride concentration at equilibrium (mg/L). K_L and Q_L are calculated by plotting of C_e/q_e vs. C_e and the data is represented in Table 3. R^2 values are very small for all the resins which indicate that the data do not fit well in the Langmuir Isotherm model.

3.2.2. Freundlich adsorption isotherm

The Freundlich equation [40] is conventionally written as:

$$\log q_e = \log K_F + \frac{1}{n_F} \log C_e \tag{6}$$

where K_F is Freundlich constant (mg/g) which indicates relative adsorption capacity and n_F is the adsorption intensity. The constants are determined by the linear plot of $\log C_e$ vs. $\log q_e$ as shown in Fig. 5. The value of the correlation coefficient (R^2) for all the resins is ≥ 0.99 . The Freundlich isotherm gives a better fit to the data than the Langmuir isotherm for fluoride adsorption. As indicated in Table 3, the values of n_F lie between 0.1 and 1 indicating a favorable adsorption.

Table 4 indicates comparative study of adsorption capacities of the ion exchangers used in the present work with the other ion exchangers used by different researchers. The adsorption capacities of resins studied are comparable with Indion FR 10 and Duolite ES 467 modified with Al^{+3} and Duolite A 171 as represented in chart. However, adsorption capacity depends on resin type, resin matrix, resin fixed ion and modified form of resin.

3.3. Study of adsorption kinetics

Kinetic study of adsorption of fluoride on different resins is carried out by using 0.2 g of resin with 10 mg/L fluoride

Table 3
Adsorption isotherms parameters for adsorption of Fluoride on different resins

Isotherm Model	Isotherm Parameters	TT-40-Al	TT-40-Fe	TT-42-Al	TT-42-Fe	TUL-10	AMB-21
Langmuir	K_L (L/mg)	0.03	-0.09	-0.19	-0.09	0.02	-0.02
	Q_L (mg/g)	16.94	-0.24	-1.22	-0.20	13.36	-5.08
	R_L	0.98	1.65	1.27	1.70	0.97	1.06
	R^2	0.076	0.963	0.620	0.769	0.089	0.164
Freundlich	K_F (mg/g)	0.49	0.02	0.29	0.02	0.28	0.13
	n_F	1.02	0.67	0.82	0.64	1.02	0.94
	R^2	0.997	0.990	0.983	0.993	0.995	0.993

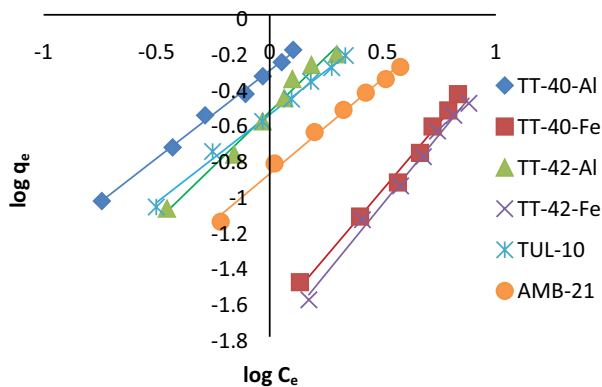


Fig. 5. Freundlich isotherm for the removal of fluoride.

solution of 50 cm³. The fluoride ion concentration in the solution after specific interval of time is checked using Orion ISE meter connected to fluoride ion selective electrode. The obtained kinetic data is studied by using following four kinetic models. Table 5 represents the correlation coefficient R^2 and rate constants.

3.3.1. Lagergren's equation for first-order kinetics

The Lagergren's equation for first-order kinetics [41] is:

$$\log(q_e - q_t) = \log q_e - \frac{k_1 t}{2.303} \quad (7)$$

where q_t is the amount of fluoride adsorbed on the resin (mg/g) at time t (min), k_1 is the Lagergren's first-order rate

constant (1/min). k_1 and q_e are calculated from the intercept and slope of the plot $\log(q_e - q_t)$ vs. t . The values are listed in Table 5 along with the R^2 values.

The R^2 values for the pseudo-first-order model are small for all the resins and the experimental q_e values and calculated q_e values by applying model are not very close which imply that the adsorption of fluoride on resins do not follow the pseudo-first-order kinetics.

3.3.2. Pseudo-second-order model

Pseudo-second-order model [42] is given as:

$$\frac{t}{q_t} = \frac{1}{k_2 q_e^2} - \frac{1}{q_e} t \quad (8)$$

where k_2 is pseudo-second-order constant (g/mg/min) and q_e which are determined experimentally from the graph of t/q_t vs. t as shown in Fig. 6 and are listed in Table 5 along with R^2 values.

The pseudo-second-order model is relevant for adsorption of fluoride on resins as the data show high correlation coefficient (≥ 0.99) for all the resins and the experimental and theoretical q_e values are in good agreement with each other. This suggests that the rate determining step may be chemisorption.

3.3.3. Ritchie's-second-order kinetic model

The modified Ritchie's-second-order kinetic model [43] is represented as:

Table 4
Comparative chart of adsorption capacities of different ion exchangers

Sl. no.	Ion exchange resins	Adsorption capacity (mg/g)	Reference
1	Strong base anion exchanger in OH ⁻ form	13.7	[22]
2	Purolite A520E	2.0	[23]
3	Duolite A 171	0.60	[24]
4	Indion FR 10	1.31	[25]
	Ceralite IRA 400	1.50	
5	Cerium-loaded poly(hydroxamic acid)	9.45	[26]
6	Lanxess TP208 resin	1.30	[27]
8	Polyacrylamide Al(III) phosphate	2.14,	[29]
	Polyacrylamide Ce(IV) phosphate	2.29	
	Polyacrylamide Zr(IV) phosphate	2.17	
9	A500P loaded with Zr	2.14	[30]
10	Amberlite 200CT modified with Al ³⁺	43.68	[31]
11	Indion FR 10 in modified with Al ³⁺	0.50	[32]
12	Aluminum complexed Duolite ES467	0.40	[33]
	TT-40-Al	0.45	
	TT-40-Fe	0.24	
	TT-42-Al	0.44	
13	TT-42-Fe	0.22	Present work
	TUL-10	0.42	
	AMB-21	0.37	

Table 5
Adsorption kinetic parameters for adsorption of fluoride on different resins

Kinetic models	Parameters	TT-40-Al	TT-40-Fe	TT-42-Al	TT-42-Fe	TUL-10	AMB-21
Pseudo-first-order	k_1 (1/min)	0.0152	0.0135	0.0215	0.0158	0.0069	0.0065
	q_e (mg/g)	1.1184	0.0741	1.9887	0.1739	0.2489	0.1566
	R^2	0.9495	0.4455	0.9803	0.7917	0.215	0.3513
Pseudo-second-order	k_2 (g/mg/min)	0.0209	0.3923	0.0086	0.2135	0.172	0.4144
	q_e (mg/g)	1.935	0.466	1.9700	0.4895	1.8615	1.3292
	h (mg/g/min)	0.0783	0.0852	0.0336	0.0511	0.5959	0.7322
	R^2	0.9979	0.9964	0.9885	0.9978	0.9971	0.9996
Ritchie's-second-order	k_R (1/min)	0.1531	0.0229	0.0722	0.0296	0.4001	0.4843
	q_e (mg/g)	1.9124	0.5123	2.0624	0.4746	2.1017	1.3752
	R^2	0.9922	0.9081	0.9843	0.9304	0.9118	0.9374
Intra-particle diffusion model	k_{id} (mg/g min ^{0.5})	0.1029	0.0138	0.1154	0.0166	0.0526	0.0215
	a	0.4591	0.2978	0.0356	0.2687	1.2665	1.0813
	R^2	0.9004	0.4773	0.9702	0.8278	0.4187	0.4737

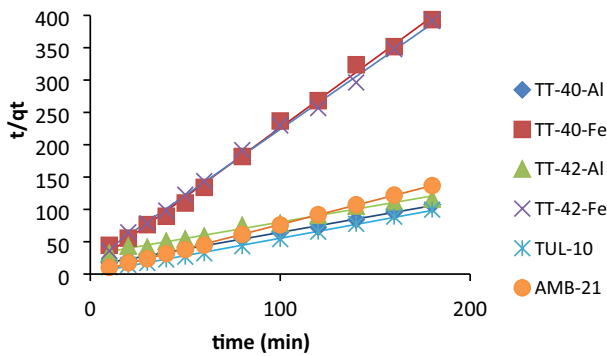


Fig. 6. Pseudo-second-order kinetic model for removal of fluoride using resins.

$$\frac{1}{q_t} = \frac{1}{k_R q_e t} + \frac{1}{q_e} \quad (9)$$

where k_R is the modified Ritchie's-second-order (1/min). k_R and q_e are obtained from the graph of $1/q_t$ vs. $1/q_e$. R^2 values are high and standardize deviation between the experimental and calculated values ($\% \Delta q$) is less. Therefore, the fluoride adsorption on resin follows modified Ritchie's-second-order kinetic model and suggests that rate limiting step may be chemical adsorption.

3.3.4. Intraparticle diffusion model

The intraparticle diffusion model [44] is expressed as:

$$q_t = k_{id} t^{0.5} + a \quad (10)$$

where k_{id} is measure of diffusion coefficient and a is intra-particle diffusion constant, an indicative of thickness of the boundary layer. By plotting a graph of q_t vs. $t^{0.5}$, constants k_{id} and a are calculated from the slope and the intercept. Fig. 7 represents the graph where the points are non-linear which indicates the lines do not pass through the origin.

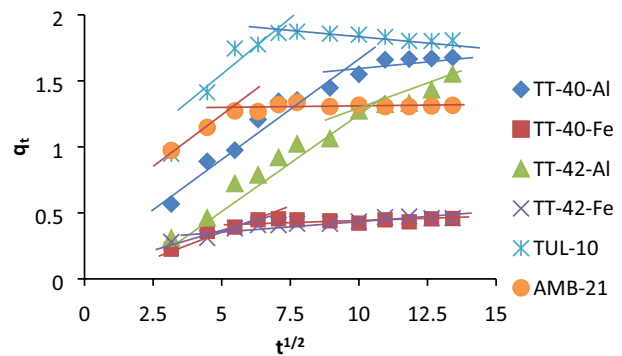


Fig. 7. Intraparticle diffusion model for the removal of fluoride.

This suggests that the intraparticle diffusion is not the only rate-limiting step [45] and the adsorption of fluoride on resins is complex. Fig. 7 depicts that in the beginning, the fluoride adsorption on resins is through surface diffusion, and later it is via intra-particle diffusion. Larger intercept values for anion exchangers TUL-10 and AMB-21 in Fig. 7 indicates that the fluoride ions get adsorbed more readily on these resins than cation exchangers [46].

3.4. Characterization of resins

3.4.1. FTIR spectroscopy analysis of resins

Figs. 8a–c represent FTIR spectra of the TT-40, TT-42, and anion exchange resins TUL-10 and AMB-21 before and after adsorption of fluoride which are recorded on a NICOLET 6700 FTIR spectrophotometer (USA) using a KBr pellet technique.

In Fig. 8a, for Al³⁺ form of TT-40 resin, the band at 3,400 cm⁻¹ is due to O–H stretching vibration, band at 1,162 cm⁻¹ is due to stretching frequency of S=O of sulfonic acid and the bands at 1,126; 1,036; and 776 cm⁻¹ corresponds to SO–Al stretching and Al–O stretching [47,48]. In Fe³⁺ form of TT-40 resin, band at 581 cm⁻¹ corresponds to the presence of Fe–O stretching [47].

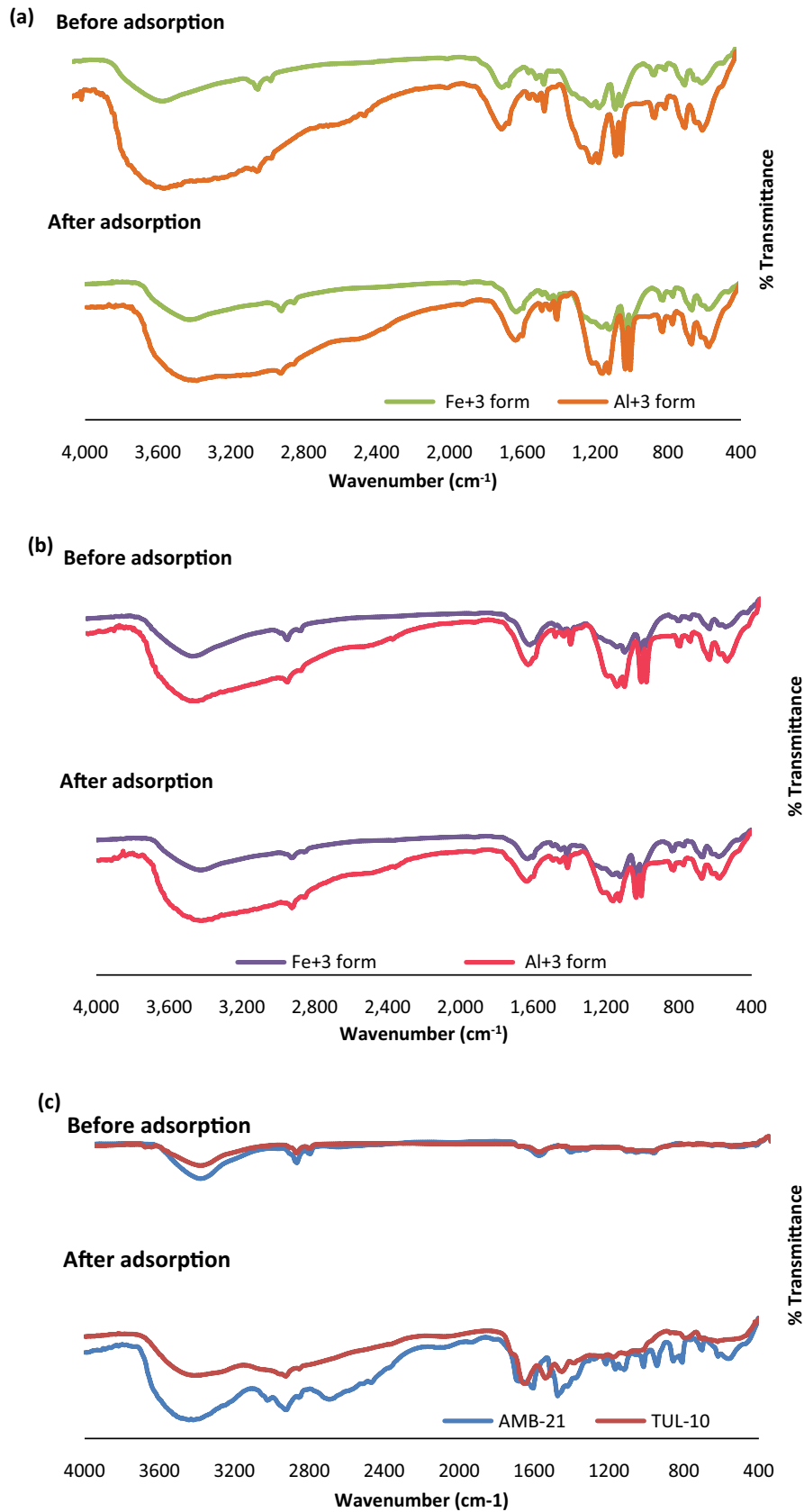


Fig. 8a. FTIR spectra of Al³⁺ and Fe³⁺ form of (a) TT-40, (b) TT-42 resins, and (c) AMB-21 and TUL-10 before and after adsorption of fluoride.

In Fig. 8b for Al^{3+} form of TT-42 resin, the band at $3,424$ and $1,164\text{ cm}^{-1}$ is due to O–H stretching vibrations and sulfonic acid group stretching vibration. Bands at $1,126$; $1,036$; and 776 cm^{-1} corresponds to SO–Al and Al–O stretching. In Fe^{3+} form of TT-42 resin, the stretching frequency at 582 cm^{-1} corresponds to the presence of Fe–O stretching.

In Fig. 8c, the band at around $1,463\text{ cm}^{-1}$ confirms the presence of tertiary amine group in AMB-21 and bands at $3,434$; $2,924$; and $2,854\text{ cm}^{-1}$ corresponds to stretching vibration of O–H group, C–H from $-\text{CH}_3$ or $-\text{CH}_2$ groups. For TUL-10, the band at $3,437\text{ cm}^{-1}$ corresponds stretching vibrations of O–H and $-\text{NH}_2$ groups and the band at $2,928\text{ cm}^{-1}$ attribute to symmetric stretch vibrations of the $-\text{CH}_2$ groups.

A broadening of O–H band in the fluoride treated resins is taken as an indicative of electrostatic adsorption between the resin and the fluoride [34].

3.4.2. SEM analysis of resins before and after adsorption

SEM images before and after fluoride adsorption of cation exchange resins TT-40-Al and TT-42-Al are shown in Figs. 9a and b, respectively. There is no much change observed in the morphology of resins after the fluoride adsorption. Similar observation is made by Li et al. [49] in adsorption studies of fluoride by using modified sludge.

3.5. Desorption study

Fig. 10 indicates that both the desorbents 0.1 N NaOH and 0.1 N HCl are efficient desorbents for anion exchangers

TUL-10, AMB-21, and cation exchangers TT-40-Fe, TT-42-Fe. However, cation exchangers TT-40-Al, TT-42-Al cannot be desorbed using any of these desorbents as fluoride forms stable fluoroalumina complex.

3.6. Field sample study

The adsorption experiments are carried out by collecting water samples from Budangad village of Bagalkot district in Karnataka, India, as fluoride content in the ground water is beyond permissible limit. The details of analysis of water sample is listed in Table 6. The fluoride adsorption experiments are carried out by taking 1 g of resin with

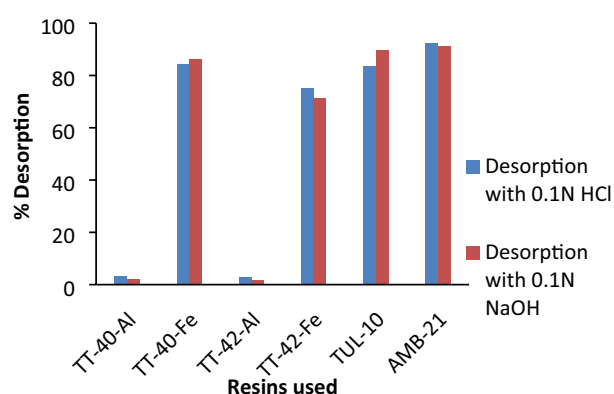


Fig. 10. Desorption study.

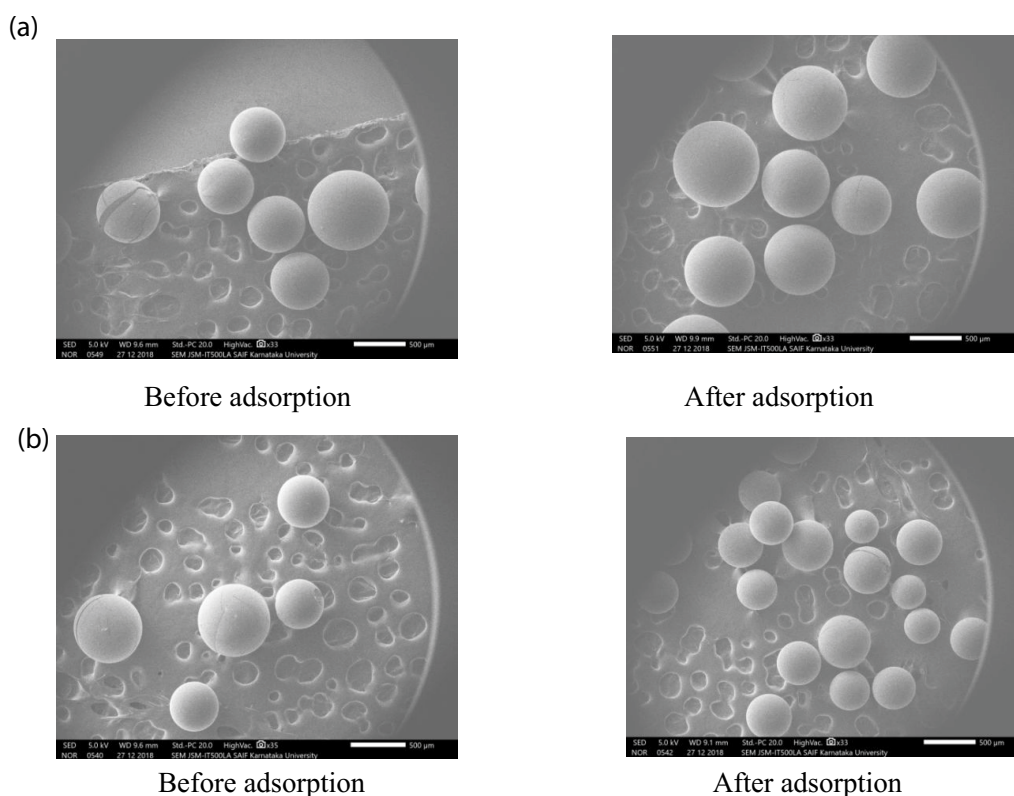


Fig. 9. SEM images of (a) TT-40-Al and (b) TT-42-Al.

Table 6

Parameters of the water sample collected from Budangad village of Bagalkot district in Karnataka, India

pH	Specific conductivity ($\mu\text{S}/\text{cm}$)	TDS (mg/L)	Hardness (mg/L)	Chloride (mg/L)	Total alkalinity (mg/L)	Fluoride (mg/L)
7.5	72.96	45.23	30.00	17.86	27.50	2.82

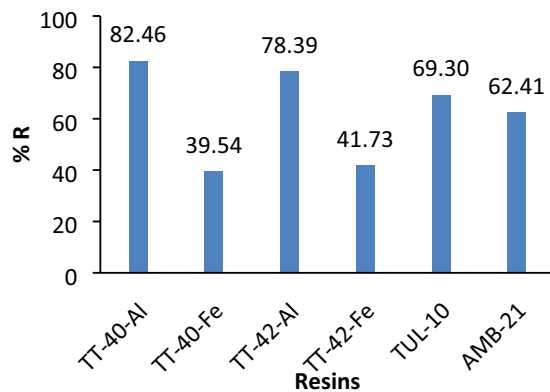


Fig. 11. Adsorption study of fluoride ions on the resins using field water sample.

50 cm³ of water sample. Fig. 11 indicates that Al⁺³ form of cation exchangers and anion exchangers are more effective for the removal of fluoride ions from the water sample. The fluoride adsorption is relatively less in water sample collected from field due to annoying ions present in the water sample.

4. Conclusions

The removal of fluoride is maximum in the pH range of 4.0–10.0 with resin quantity of 0.2 g. Maximum removal of fluoride is observed within 60 min for anion exchangers and 120 min for cation exchangers. The experimental data fit well in Freundlich isotherm. The kinetic study suggests adsorption process follows pseudo-second-order reaction kinetics. Among two anion exchangers used for the removal of fluoride TUL-10 has better fluoride removal efficiency than AMB-21 as TUL-10 has hydrophilic acrylic matrix, however in case of modified cation exchangers Al⁺³ form of resins has better fluoride removal efficiency than Fe⁺³ form. This clearly indicates modified resins can be used for removal of fluoride. Desorption of resins with 0.1N HCl and 0.1 N NaOH clearly indicates desorption is possible in case of anion exchangers and cation exchangers in Fe⁺³ form. Effectiveness of the resins for the removal of fluoride by adsorption process is also tested for field samples.

References

- [1] Indian Standard, Drinking Water Specification, Second Revision, IS-10500, 2012.
- [2] S. Jagtap, M.K. Yenkie, N. Labhsetwar, S. Rayalu, Fluoride in drinking water and defluoridation of water, *Chem. Rev.*, 112 (2012) 2454–2466.
- [3] D. Kanduti, P. Sterbenk, B. Artnik, Fluoride: a review of use and effects on health, *Mater. Sociomed.*, 28 (2016) 2016133–2016137.
- [4] M.G. Sujana, R.S. Thakur, S.B. Rao, Removal of fluoride from aqueous solution by using alum sludge, *J. Colloid Interface Sci.*, 206 (1998) 94–101.
- [5] M. Islam, R.K. Patel, Evaluation of removal efficiency of fluoride from aqueous solution using quick lime, *J. Hazard. Mater.*, 143 (2007) 303–310.
- [6] S. Ghorai, K.K. Pant, Equilibrium, kinetics and breakthrough for adsorption of fluoride on activated alumina, *Sep. Purif. Technol.*, 42 (2004) 265–271.
- [7] S.S. Tripathy, J.L. Bersillon, K. Gopal, Removal of fluoride from drinking water by adsorption onto alum-impregnated activated alumina, *Sep. Purif. Technol.*, 50 (2006) 310–317.
- [8] S.M. Maliyekkal, S. Shukla, L. Philip, I.M. Nambi, Enhanced fluoride removal from drinking water by magnesia-amended activated alumina granules, *Chem. Eng. J.*, 140 (2008) 183–192.
- [9] T. Getachew, A. Hussien, V.M. Rao, Defluoridation of water by activated carbon prepared from banana (*Musa paradisiaca*) peel and coffee (*Coffea arabica*) husk, *Int. J. Environ. Sci. Technol.*, 12 (2015) 1857–1866.
- [10] R. Sivabalan, S. Rengaraj, B. Arabindoo, V. Murugesan, Fluoride uptake characteristics of activated carbon from agricultural waste, *J. Sci. Ind. Res.*, 61 (2002) 1039–1045.
- [11] N.A. Medellin-Castillo, R. Leyva-Ramos, R. Ocampo-Perez, R.F. Garcia de la Cruz, A. Aragon-Piña, J.M. Martinez-Rosales, R.M. Guerrero-Coronado, L. Fuentes-Rubio, Adsorption of fluoride from water solution on bone char, *Ind. Eng. Chem. Res.*, 46 (2007) 9205–9212.
- [12] S. Patnaik, P.C. Mishra, R.N. Nayak, A.K. Giri, Removal of fluoride from aqueous solution using chitosan-iron complex, *J. Anal. Bioanal. Tech.*, 7 (2016) 326–333.
- [13] N. Chen, Z.Y. Zhang, C.P. Feng, M. Li, R.Z. Chen, N. Sugiura, Investigations on the batch and fixed-bed column performance of fluoride adsorption by Kanuma mud, *Desalination*, 268 (2011) 76–82.
- [14] M.K. Adak, B. Mondal, P. Dhak, S. Sen, D. Dhak, A comparative study on fluoride removal capacity from drinking water by adsorption using nano-sized alumina and zirconia modified alumina prepared by chemical route, *Adv. Water Sci. Technol.*, 4 (2017) 1–10.
- [15] L. Chen, B.Y. He, S. He, T.J. Wang, C.L. Su, Y. Jin, Fe–Ti oxide nano-adsorbent synthesized by co-precipitation for fluoride removal from drinking water and its adsorption mechanism, *Powder Technol.*, 227 (2012) 3–8.
- [16] L. Jayarathna, A. Bandara, W.J. Ng, R. Weerasooriya, Fluoride adsorption on $\gamma\text{-Fe}_2\text{O}_3$ nanoparticles, *J. Environ. Health Sci. Eng.*, 13 (2015) 1–10.
- [17] M. Bhaumik, T.Y. Leswif, A. Maity, V.V. Srinivasu, M.S. Onyango, Removal of fluoride from aqueous solution by polypyrrole/Fe₃O₄ magnetic nanocomposite, *J. Hazard. Mater.*, 186 (2011) 150–159.
- [18] C.K. Diawara, S.N. Diop, M.A. Diallo, M.A. Farcy, Determination performance of nanofiltration (NF) and low pressure reverse osmosis (LPRM) membranes in the removal of fluorine and salinity from Brackish drinking water, *J. Water Resour. Prot.*, 3 (2011) 912–917.
- [19] I. Bejaoui, A. Mnif, B. Hamrouni, Performance of reverse osmosis and nanofiltration in the removal of fluoride from model water and metal packaging industrial effluent, *Sep. Sci. Technol.*, 49 (2014) 1135–1145.
- [20] M. Arda, E. Orhan, O. Arar, M. Yuksel, N. Kabay, Removal of fluoride from geothermal water by electrodialysis, *Sep. Sci. Technol.*, 44 (2009) 841–853.
- [21] K. Majewska-Nowak, M. Grzegorzczek, M. Kabsch-Korbutowicz, Removal of fluoride ions by batch electrodialysis, *Environ. Prot. Eng.*, 41 (2015) 67–81.

- [22] M.T. Samadi, M.N. Sepehr, M. Zarrabi, S.M. Ramhormozi, S. Azizan, A. Amrane, Removal of fluoride ions by ion exchange resin: kinetic and equilibrium studies, *Environ. Eng. Manage. J.*, 13(2014) 205–214.
- [23] A.B. Nasr, C. Charcosset, R.B. Amar, K. Walha, Fluoride removal from aqueous solution by Purolite A520E resin: kinetic and thermodynamics study, *Desal. Water Treat.*, 54 (2015) 1604–1611.
- [24] M.R. Gandhi, G. Kalaivani, S. Meenakshi, Sorption of chromate and fluoride onto duolite a 171 anion exchange resin - a comparative study, *Elixir Poll.*, 32 (2011) 2034–2040.
- [25] S. Meenakshi, N. Viswanathan, Identification of selective ion-exchange resin for fluoride sorption, *J. Colloid Interface Sci.*, 308 (2007) 438–450.
- [26] M.J. Haron, W.M.Z. Wan Yunus, Removal of fluoride ion from aqueous solution by a cerium-poly(hydroxamic acid) resin complex, *J. Environ. Sci. Health., Part A*, 36 (2001) 727–734.
- [27] G.J. Millar, S.J. Couperthwaite, D.B. Wellner, D.C. Macfarlane, S.A. Dalzell, Removal of fluoride ions from solution by chelating resin with imino-diacetate functionality, *J. Water Process. Eng.*, 20 (2017) 113–122.
- [28] I.B. Solangi, S. Memon, M.I. Bhangar, Removal of fluoride from aqueous environment by modified Amberlite resin, *J. Hazard. Mater.*, 171 (2009) 815–819.
- [29] C.S. Sundaram, S. Meenakshi, Fluoride sorption using organic-inorganic hybrid type ion exchangers, *J. Colloid Interface Sci.*, 333 (2009) 58–62.
- [30] O. Hakami, New hybrid anion exchanger for fluoride removal, *Nat. Environ. Pollut. Technol.*, 16 (2017) 653–658.
- [31] F. Luo, K. Inoue, The removal of fluoride ion by using metal(III)-loaded amberlite resins, *Solvent Extr. Ion Exch.*, 22 (2004) 305–322.
- [32] N. Viswanathan, S. Meenakshi, Role of metal ion incorporation in ion exchange resin on the selectivity of fluoride, *J. Hazard. Mater.*, 162 (2009) 920–930.
- [33] D.B. Bhatt, P.R. Bhatt, H.H. Prasad, K.M. Papat, P.S. Anand, Removal of fluoride ion from aqueous bodies by aluminium complexed amino phosphonic acid type resins, *Indian J. Chem. Technol.*, 11 (2004) 299–303.
- [34] S.M. Prabhu, S. Meenakshi, Effect of metal ions loaded onto iminodiacetic acid functionalized cation exchange resin for selective fluoride removal, *Desal. Water Treat.*, 52 (2014) 2527–2536.
- [35] N.K. Mondal, R. Bhaumik, J.K. Datta, Removal of fluoride by aluminum impregnated coconut fiber from synthetic fluoride solution and natural water, *Alex. Eng. J.*, 54 (2015) 1273–1284.
- [36] A.B. Nasr, K. Walha, C. Charcosset, R.B. Amar, Removal of fluoride ions using cuttlefish bones, *J. Fluorine Chem.*, 132 (2011) 57–62.
- [37] C. Zhang, Y. Li, T.J. Wang, Y. Jiang, H. Wang, Adsorption of drinking water fluoride on a micron-sized magnetic Fe_3O_4 @Fe-Ti composite adsorbent, *Appl. Surf. Sci.*, 363 (2016) 507–515.
- [38] H. Mittal, V. Kumar, Saruchi, S.S. Ray, Adsorption of methyl violet from aqueous solution using gum xanthan/ Fe_3O_4 based nanocomposite hydrogel, *Int. J. Biol. Macromol.*, 89 (2016) 1–11.
- [39] J. Zhang, N. Chen, Z. Tang, Y. Yu, Q. Hu, C. Feng, A study of the mechanism of fluoride adsorption from aqueous solutions onto Fe-impregnated chitosan, *Phys. Chem. Chem. Phys.*, 17 (2015) 12041–12050.
- [40] M.E. Ravančić, M. Habuda-Stanić, Equilibrium and kinetics studies for the adsorption of fluoride onto commercial activated carbons using fluoride ion selective electrode, *Int. J. Electrochem. Sci.*, 10 (2015) 8137–8149.
- [41] S. Omid, A. Kakanejadifard, Eco-friendly synthesis of graphene–chitosan composite hydrogel as efficient adsorbent for Congo red, *RSC Adv.*, 8 (2018) 12179–12189.
- [42] Saruchi, V. Kumar, B.S. Kaith, R. Jindal, Synthesis of hybrid ion exchanger for rhodamine B dye removal: equilibrium, kinetic and thermodynamic studies, *Ind. Eng. Chem. Res.*, 55 (2016) 10492–10499.
- [43] A. Kara, E. Demirbel, Kinetic, isotherm and thermodynamic analysis on adsorption of Cr(VI) ions from aqueous solutions by synthesis and characterization of magnetic-poly(divinylbenzene-vinylimidazole) microbeads, *Water Air Soil Pollut.*, 223 (2012) 2387–2403.
- [44] J. Liu, L. Wu, X. Chen, Kinetic model investigation on lead(II) adsorption using silica-based hybrid membranes, *Desal. Water Treat.*, 54 (2015) 2307–2313.
- [45] Saruchi, V. Kumar, Adsorption kinetics and isotherms for the removal of rhodamine B dye and Pb^{2+} ions from aqueous solutions by a hybrid ion-exchanger, *Arabian J. Chem.*, 12 (2019) 316–329.
- [46] J.M. Karekar, S.V. Divekar, Removal of thiocyanate from water by using weak base microporous resins of different matrix structure, *Desal. Water Treat.*, 167 (2019) 176–182.
- [47] M.K. Adak, S. Chakraborty, S. Sen, D. Dhak, Synthesis and optimization of low cost and high efficient zirconium aluminium modified iron oxide nano adsorbent for fluoride removal from drinking water, *Adv. Mater. Proc.*, 2 (2017) 716–724.
- [48] S. Tandorn, O.A. Arquerpanyo, W. Naksata, P. Sooksamiti, Preparation of anion exchange resin loaded with ferric oxide for arsenic(V) removal from aqueous solution, *Int. J. Environ. Sci. Dev.*, 8 (2017) 399–403.
- [49] Y. Li, S. Yang, Q. Jian, J. Fang, W. Wang, Y. Wang, The adsorptive removal of fluoride from aqueous solution by modified sludge: optimization using response surface methodology, *Int. J. Environ. Res. Public Health*, 15 (2018) 1–14.